J Neurophysiol 98: 2223–2231, 2007.
First published August 22, 2007; doi:10.1152/jn.00722.2007.

Crossed Commissural Pathways in the Spinal Hindlimb Enlargement Are Not Necessary for Right–Left Hindlimb Alternation During Turtle Swimming

Ramsey F. Samara and Scott N. Currie
Department of Cell Biology and Neuroscience, University of California, Riverside, Riverside, California

Submitted 27 June 2007; accepted in final form 19 August 2007

Samara RF, Currie SN. Crossed commissural pathways in the spinal hindlimb enlargement are not necessary for right–left hindlimb alternation during turtle swimming. *J Neurophysiol* 98: 2223–2231, 2007. First published August 22, 2007; doi:10.1152/jn.00722.2007. We examined the coordination between right and left hindlimbs during voluntary forward swimming in adult red-eared turtles, before and after midsagittal section of the spinal cord hindlimb enlargement (segments D8–S2) or the enlargement plus the first preenlargement segment (D7–S2). Our purpose was to assess the role of crossed commissural axons in these segments for right–left hindlimb alternation during voluntary locomotion. Midsagittal splitting severed commissural fibers and separated the right and left halves of the posterior spinal cord. Adult turtles ($n = 9$) were held by a band clamp around the shell in a water-filled tank while digital video of forward swimming was recorded from below and computer analyzed with motion analysis software. In a subset of these animals ($n = 5$), we also recorded electromyograms from hip extensor and/or hip flexor muscles on both sides. Surprisingly, splitting spinal segments D8–S2 or D7–S2 did not affect the strength of out-of-phase coordination between right and left hindlimbs, although hindlimb movement amplitudes were reduced compared with presurgical controls. These results show that commissural axons in the hindlimb enlargement and preenlargement cord are not necessary for right–left hindlimb alternation during voluntary swimming. We suggest that alternating propriospinal drive from the right and left sides of the forelimb enlargement maintains the out-of-phase coordination of right and left hindlimbs in the bisected-cord preparation. Our data support the hypothesis that descending propriospinal (forelimb–hindlimb) and crossed commissural (hindlimb–hindlimb) spinal cord pathways function together as redundant mechanisms to sustain right–left hindlimb alternation during turtle locomotion.

INTRODUCTION

Production of vertebrate locomotor behavior depends on the rhythmic activity of central pattern generator (CPG) neuronal networks in the spinal cord. These networks produce motor output to limb and trunk musculature consisting of proper rostrocaudal and right–left coordination according to an animal's needs (for review, see Butt et al. 2002; Kiehn 2006; Roberts et al. 1998; Stein et al. 1997). During locomotor behavior, CPGs may be required to produce synchronized (in-phase) motor output between the right and left sides of the body, such as that seen in flying (locust: Wendler 1977; Wilson 1961; goose: Sholomenko et al. 1991), galloping (cat: English 1979; Miller et al. 1975), hopping (frog: Peters et al. 1996; rat-kangaroo: Webster and Dawson 2003), and fast swimming in frogs (Ostry et al. 1991; Peters et al. 1996); or to produce alternating (out-of-phase) motor output between the right and left sides, as in swimming (newt: Delvolve et al. 1997; lamprey: Cohen and Wallen 1980; Poon 1980; *Xenopus* embryo: Kahn et al. 1982; turtle: Field and Stein 1997; fish: Masino and Fetcho 2005) and walking (cat: Miller et al. 1975; turtle: Walker 1971; goose: Sholomenko et al. 1991; chick: Jacobson and Hollyday 1982). During locomotion, out-of-phase side-to-side coordination is carried out at least in part by spinal commissural pathways because disruption of these pathways by photoinactivation (lamprey: Buchanan and McPherson 1995), midsagittal spinal lesions (*Xenopus* embryo: Kahn and Roberts 1982; lamprey: Cangiano and Grillner 2003; neonatal rat: Kjaerulff and Kiehn 1996), or application of the glycine receptor antagonist strychnine (lamprey: Cohen and Harris-Warrick 1984; Hagevik and McClellan 1994; McPherson et al. 1994; mudpuppy: Jovanovic et al. 1999; neonatal rat: Juvin et al. 2005) disrupts right–left alternation. However, other studies indicate that descending propriospinal pathways can play an important role in maintaining proper right–left alternation of locomotor output under some conditions (cat: Kato 1988; *Xenopus* embryo: Soffe and Roberts 1982; lamprey: Jackson et al. 2005; neonatal rat: Cowley and Schmidt 1997; Kremer and Lev-Tov 1997).

Although most previous work assessed the role of commissural pathways in side-to-side alternation during electrically or chemically evoked motor patterns in reduced preparations, our study investigates coordinating mechanisms in the turtle spinal cord during *voluntary* locomotion in otherwise intact animals. Voluntary forward swimming in freshwater turtles typically consists of 1:1 out-of-phase movement of contralateral limbs (right–left forelimbs: RF–LF; and right–left hindlimbs: RH–LH) and of ipsilateral limbs (RF–RH and LF–LH), and 1:1 nearly in-phase movement of diagonal limbs (RF–LH and LF–RH) (Davenport et al. 1984; Field and Stein 1997; Gillis and Blob 2001; Stein 1978; Zug 1971), similar to the interlimb coordination seen during trot in quadruped mammals (Hildebrand 1989). During the normal hindlimb forward swim motor pattern, hip extensor electromyographic discharge alternates with ipsilateral hip flexor activity and contralateral hip extensor activity (Earhart and Stein 2000; Stein 2005). To assess the necessity of commissural axons in the hindlimb enlargement (spinal segments D8–S2) or the hindlimb enlargement plus the first preenlargement segment (D7–S2) for maintaining right–left hindlimb alternation during voluntary forward swimming, we measured interlimb phase before and after bisection of these segments. Preliminary results have been published in abstract form (Samara and Currie 2005).

Address for reprint requests and other correspondence: S. N. Currie, Department of Neuroscience, University of California, Riverside, CA 92521 (E-mail: currie@mail.ucr.edu).

The costs of publication of this article were defrayed in part by the payment of page charges. The article must therefore be hereby marked "*advertisement*" in accordance with 18 U.S.C. Section 1734 solely to indicate this fact.

METHODS

Spinal cord exposure and deafferentation

Red-eared turtles, *Trachemys scripta elegans* ($n = 9$), with plastron lengths of 12–16 cm, were placed in crushed ice for at least 2 h before surgery to induce hypothermic anesthesia (Lennard and Stein 1977). Turtles remained partially submerged in ice for all surgical procedures. The hindlimb-region spinal cord was exposed from segments D6–S2 by dorsal laminectomy and transected at the posterior end of S2. In six turtles, bilateral dorsal rhyzotomies were performed to deafferent segments D8–S2 ($n = 1$) or D7–S2 ($n = 5$) at the start of the experiment, before prebisection behavioral testing. Three turtles were not deafferented before prebisection testing because this procedure tended to decrease swimming activity. One of the turtles in this group was deafferented after the D7–S2 cord bisection. All cord exposures were covered with dental utility wax (Heraeus Kulzer, South Bend, IN), glued to the surrounding shell with Permabond adhesive.

Movement and EMG recording

We videotaped turtle swimming from below by a horizontal digital video camera (Canon Optura 20 mini-DV), aimed at a 45° mirror beneath the clear Plexiglas bottom of the swim tank [Fig. 1*A*; tank measurements: 40 × 35 × 16 cm (length × width × height)]. Brightly colored markers (3-mm plastic beads) were sutured to the skin at the ventral–medial side of the wrists (*h* and *i* in Fig. 1*B*) and the ventral–anterior side of the knees (*f* and *g*) to track movement of the limbs relative to fixed reference points that were painted on the ventral plastron with white Liquid Paper correction fluid (*a–e*). Reference points *a* and *c* in Fig. 1*B* marked the rostral and caudal ends of the ventral midline; *b* marked the rostrocaudal level of the anterior border of the lateral shell bridge and an approximate pivot point of the pectoral girdle; *d* and *e* marked the positions of the right and left hip joints, respectively (note that images were inverted in the mirror). Video recordings were obtained with a 30-Hz frame rate and 1/250-s shutter speed, and were reviewed and annotated with a Sony GV-1000 Video Walkman. Selected swim episodes were then viewed frame by frame on a laboratory PC so that marker locations on the limbs and plastron could be manually digitized with Motus 8 software (Peak Performance Technologies, Englewood, CO). The same software was used to calculate limb movement amplitudes and interlimb phase values. We defined *cycle onsets* and *cycle offsets* in hip and forelimb movement recordings as the minimum (peak flexed) and maximum (peak extended) limb angles, respectively (Field and Stein 1997; Stein 1978). *Hip angle* was defined as the angle between the thigh line (*d–f* on the right or *e–g* on the left in Fig. 1*B*) and a line parallel to the ventral midline (*a–c*) with its origin at the hip joint (dashed line in Fig. 1*B*). The hip joint (acetabulum) is relatively fixed in the horizontal plane, even during the large pelvic girdle rotations that accompany vigorous locomotion (Walker 1971; PSG Stein, RF Samara, and SN Currie, unpublished observations). *Forelimb angle* was defined as $\angle abh$ on the right and $\angle abi$ on the left, and was measured relative to a stationary point on the ventral midline (*b*; see earlier text); this point corresponded to the rostrocaudal level of right and left pivot points on the pectoral girdle, where the scapular prongs articulate with the dorsal carapace (Walker 1971). We used this arbitrarily defined "forelimb angle" rather than "shoulder angle" because the shoulder joint (glenoid cavity) is not fixed during turtle locomotion, but moves through an arc between anterolateral and lateral positions as the pectoral girdle rotates (Walker 1971). Without X-ray cinematography, we were thus unable to estimate the position of the shoulder joint in video images. *Head angle* was defined as $\angle abj$, where an angle of 0° indicated that the head was pointed straight forward and positive or negative angles indicated that the head was turned to the right or left, respectively.

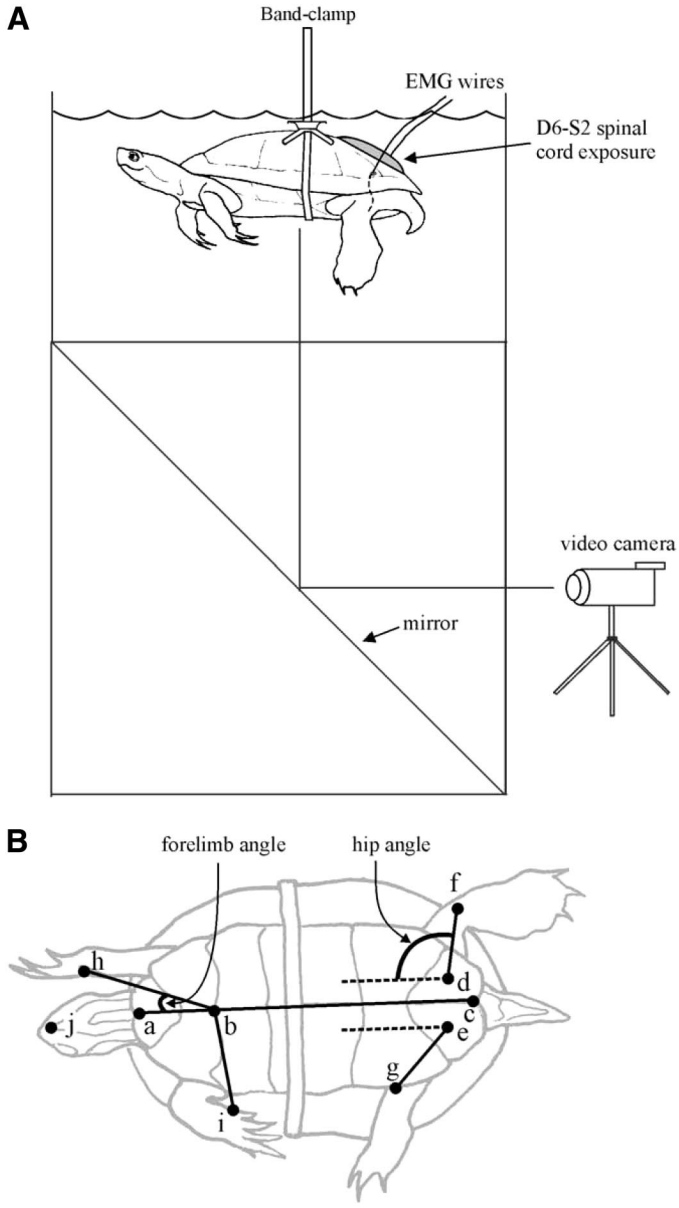

FIG. 1. Experimental setup. *A*: turtles were held by band clamp in a Plexiglas water-filled tank and allowed to swim voluntarily. They were videotaped from below in a mirror placed at 45° relative to the clear tank bottom using a digital camera (frame rate = 30 Hz, shutter speed = 1/250 s) while electromyograms (EMGs) were recorded from right and left hindlimb muscles (hip extensors and/or hip flexors). *B*: ventral view showing the location of plastron, limb, and chin markers used to obtain hip, forelimb, and head angles. Markers were painted on the plastron midline at the anterior and posterior margins (*a* and *c*, respectively), as well as the border of the humeral and pectoral plates (*b*), marks the rostrocaudal level of the anterior border of the lateral shell bridge and a pivot point of the pectoral girdle corresponding to the approximate rostrocaudal (but not lateral) position of the right and left pectoral girdle pivot points (see METHODS). Markings were also placed at the estimated locations of right and left hips (*d* and *e*, respectively). Fluorescent beads were bilaterally sewn to the skin on the ventral surfaces of the knees (*f* and *g*), wrists (*h* and *i*), and ankles (not shown).

Electromyograms (EMGs) were recorded with bipolar electrodes consisting of two 0.004-in. silver wires (California Fine Wire Company, Grover City, CA) glued together with Permabond 910 adhesive (National Starch and Chemical, Bridgewater, NJ). EMG electrodes were implanted bilaterally into hip extensor muscles (HE: flexor cruris pars flexor tibialis internus; $n = 3$), hip flexor muscles (HF: pubois-

chiofemoralis internus pars anteroventralis; $n = 1$), or both ($n = 1$; Robertson et al. 1985; Walker 1973), using previously described techniques (Earhart and Stein 2000). EMGs were amplified, filtered (30–1,000 Hz), digitized (PCM Model 3000A, Vetter), and stored on VHS videotape with a voice channel and synchronization marker (see following text). Swim episodes with EMGs were used only if they exhibited distinct bursts of muscle activity followed by periods of quiescence for a minimum of four consecutive cycles. Episodes chosen for figures were formatted with Datapac 2K2 (Run Technologies, Laguna Hills, CA) and CorelDraw (Corel, Ottawa, Canada) software.

A remote video synchronization unit (Peak Performance Technologies) was used to synchronize EMG recordings with kinematic video data. When manually activated, the synchronization unit produced a voltage deflection on an unused channel of the EMG record and a simultaneous sound pulse on the microphone input of the digital video camera. The kinematic sequence containing the onset of the sound pulse was marked and synchronized with the corresponding EMG recording in CorelDraw.

Bisections

We longitudinally bisected the dorsally exposed spinal cord from segments D7–S2 or D8–S2 (Fig. 2). Bisections were performed by first perforating the pia mater with fine iridectomy scissors at the anterior side of the exposure, then cutting posteriorly down the midline along the visible midsagittal sulcus. A #11 scalpel was then passed down this initial scissor cut until the right and left halves of the cord were completely separated over the specified region.

Histology

At the end of each experiment, turtles were reanesthetized in crushed ice and the D6–S2 cord was removed and placed in 4% paraformaldehyde for approximately 1 wk. After cord removal, turtles were killed by freezing. Cords were sectioned in the transverse plane (80 μm), mounted, and allowed to dry overnight. The next day, sections were stained with 0.1% cresyl echt violet (CellPoint Scientific, Rockville, MD) and coverslipped. Several sections were mounted from each of the seven exposed spinal segments, to verify the longitudinal extent, lateral position, and completeness of the D7–S2 or D8–S2 bisection (Fig. 2). Selected sections were photographed with a Nikon Microphot FX-A microscope using bright-field illumination.

Data analysis

The same 25 forward swim cycles were analyzed for both phase and amplitude parameters. Selected digitized episodes, in the form of time-varying angle measurements, were exported from Motus 8 as ASCII files and imported into Datapac 2K2 for further analyses. Because turtles restrained by band clamp rarely swim for extended periods, particularly after spinal surgery, we accepted swim episodes consisting of four or more cycles. The first cycle and last cycle were never quantitatively analyzed because their amplitudes were rarely representative of the entire swim episode.

Dual-referent interlimb phase values were calculated with Datapac 2K2 because dual-referent analysis is appropriate for cyclical behaviors that exhibit variable duty cycles (Berkowitz and Stein 1994; Field and Stein 1997). For this purpose, one limb was selected as "referent" (RF or RH) and the other as "target." The onsets of referent-limb extension were defined by phase values of 0.0 and 1.0. The offsets of referent extension (onsets of referent flexion) were defined by a phase value of 0.5 (for a more detailed description of phase calculations see Field and Stein 1997). To rule out the possibility of phase drift, we analyzed phase as a function of time over the course of many swim episodes (data not shown). Interlimb phase values were always similar between the early and late swim cycles for any given episode; there was no evidence of drift. Circular statistics (Batschelet 1981; Mardia and Jupp 2000; Zar 1999) and plots were calculated for phase data using Oriana 2.0 software (Kovach Computing Services, Anglesey, Wales, UK). The Rayleigh test used vector length to determine whether phase distributions were significantly clustered around the mean (nonuniform). In addition to obtaining these statistics for individual turtles, prebisection and postbisection phase values were each pooled across experiments for turtles that received the same surgical

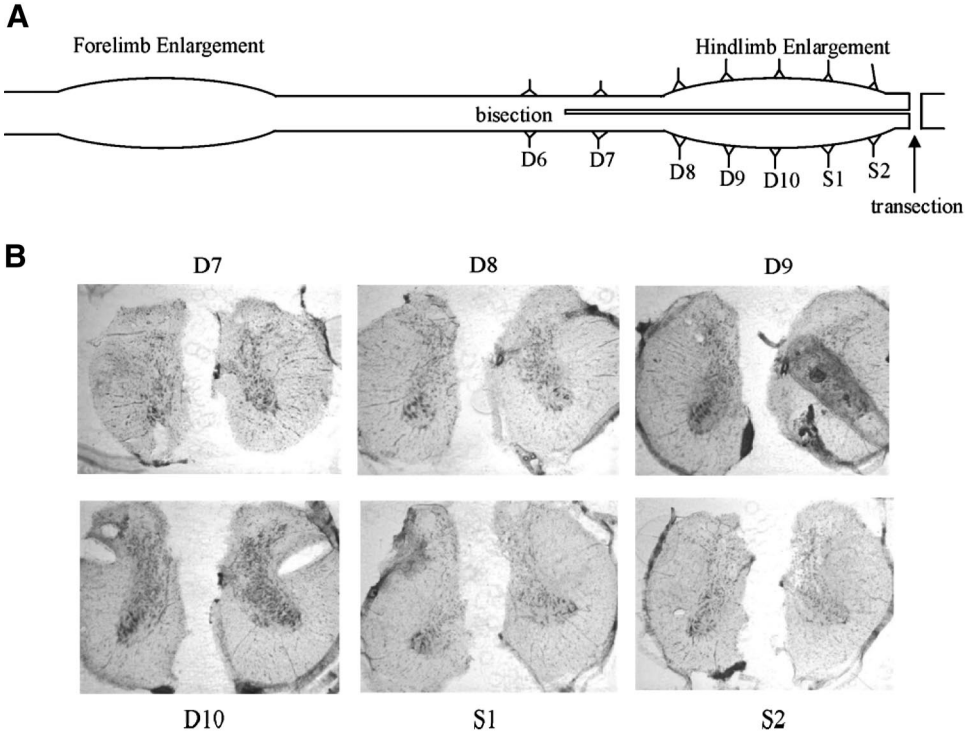

FIG. 2. Location and histological verification of spinal cord bisections. *A*: cords were split down the longitudinal midline from segments D8–S2 or D7–S2 (shown) after behavioral testing. Transections were performed before behavioral testing during the initial cord exposure. Spinal cord exposures contained only the labeled segments (D6–S2). *B*: cresyl echt violet was used to verify that bisections down the midline spanned the entire dorsoventral axis. One representative section from each segment is shown, all from the same turtle (R100).

manipulations (D7–S2 or D8–S2 cord bisection, afferented or deafferented). Mean phase and circular SD were calculated for these pooled data (Table 1). The Watson–Williams test was used to determine whether postbisection mean phase values were significantly different from prebisection means (Batschelet 1981; Zar 1999).

Amplitude was measured in Datapac 2K2 by subtracting the minimum hip or forelimb angle from the maximum angle for each cycle (peak to peak). The plastron was always kept as close as possible to the horizontal plane during swim sequences. To determine whether limb movements were planar, we measured the distance between two plastron markers (*b–c* in Fig. 1*B*) and the distance between hip and knee markers ("thigh-length": *d–f* on the right, *e–g* on the left) by hand on stationary (hypothermic) turtles in some experiments. The actual ratio of thigh length on the right and left to the fixed plastron measurement (*b–c*) was calculated based on these measurements. The same ratio was calculated by Motus 8 software using the location of digitized markers throughout the videotaped swim cycle. We compared the two values (actual vs. digitized length ratios), and found that digitized length ratios were always ≥70% of the actual ratio for a given turtle, meaning that the thigh stayed within 70% of the horizontal plane throughout the swim sequence. Pre- and postbisection data were normalized to the mean prebisection amplitude for each limb then pooled together across experiments based on which surgical procedures were performed. Mean amplitude and SD were obtained for these pooled, normalized data. The Mann–Whitney *U* test was used to determine whether pre- and postbisection amplitudes were significantly different (Table 2).

RESULTS

Swimming before spinal cord bisections

PHASE ANALYSIS. Forward swim episodes were analyzed only if they exhibited *1*) out-of-phase 1:1 forelimb movements on the right and left sides with interlimb phase values between 0.4 and 0.6; *2*) a forelimb cycle period no greater than 1.5 s; and *3*) a head angle no greater than ±10° off-center to the right or left, which indicated that the turtle was attempting to swim forward and not turn. Using these criteria in swimming prebisection turtles, contralateral hindlimbs (LH–RH) always displayed strong out-of-phase coordination with mean phase values close to 0.5 (range = 0.47–0.53; Table 1). Ipsilateral forelimb–hindlimb pairs (RH–RF) were also out of phase, with mean phase values near 0.4 (range = 0.40–0.43), whereas diagonal limbs (LH–RF) were nearly in phase for every turtle, with mean phase values close to 1.0 (range = 0.89–0.95). We used circular statistics to evaluate the degree of clustering or directionality of phase measurements. The Rayleigh statistic tests the hypothesis that a circular distribution is nonuniform (i.e., significantly clustered around a mean value). For every turtle in the present study, the distribution of phase values was clustered for all four sets of measurements (LH–RH, LF–RF, RH–RF, and LH–RF; $P < 0.0001$). In determining the degree of clustering for a set of data points, the Rayleigh test uses the length of the mean vector (**r**), which ranges from 0 to 1. A vector length of 0 signifies no coupling between limbs, whereas a length of 1 signifies perfect coupling (Batschelet 1981). For each prebisection turtle, limbs were strongly coupled, with vector lengths ranging from 0.84 to 0.98 (LH–RH), 0.91–0.98 (LF–RF and LH–RF), and 0.85–0.99 (RH–RF) (Figs. 3 and 4). Bursts of EMG activity were closely correlated with motion data, with HE burst onsets occurring near the minimum hip angle (peak hip flexion) for each cycle and HF burst onsets occurring near the maximum hip angle (peak hip extension) for each cycle.

AMPLITUDE ANALYSIS. For individual prebisection turtles, mean forelimb movement amplitudes ranged between 71.0 ± 5.0 and 93.8 ± 7.6°, peak to peak. Mean hip excursions ranged from 43.5 ± 22.4 to 102.4 ± 16.6°. For purposes of comparison with postbisection data, pooled forelimb and hip amplitude data were both normalized, resulting in prebisection means of 100.0 for all four measures (right forelimb, left forelimb, right hip, left hip) (Table 2).

Swimming after D8–S2 and D7–S2 spinal cord bisections

PHASE ANALYSIS. We tested the necessity of commissural axons in the hindlimb enlargement for out-of-phase coordina-

TABLE 1. *Interlimb phase before and after cord bisections in afferented and deafferented animals*

	Animals/Cycles	LH–RH	LF–RF	LH–RF	RH–RF
		A. Afferented animals			
D8–S2 bisections					
Prebisection	1/25	0.53 ± 0.05	0.52 ± 0.06	0.94 ± 0.04	0.40 ± 0.04
Postbisection	1/25	0.42 ± 0.04*	0.55 ± 0.05	0.92 ± 0.06	0.48 ± 0.07*
D7–S2 bisections					
Prebisection	3/75	0.49 ± 0.08	0.50 ± 0.06	0.89 ± 0.06	0.41 ± 0.07
Postbisection	3/75	0.45 ± 0.07*	0.49 ± 0.07	0.91 ± 0.10	0.42 ± 0.09
		B. Deafferented animals			
D8–S2 bisections					
Prebisection	4/100	0.47 ± 0.09	0.51 ± 0.05	0.91 ± 0.08	0.41 ± 0.06
Postbisection	4/100	0.48 ± 0.07	0.49 ± 0.05*	0.92 ± 0.09	0.38 ± 0.11*
D7–S2 bisections					
Prebisection	3/75	0.47 ± 0.10	0.53 ± 0.06	0.93 ± 0.10	0.43 ± 0.05
Postbisection	3/75	0.51 ± 0.13*	0.49 ± 0.09*	0.90 ± 0.14	0.33 ± 0.06*

Animals/Cycles refers to the number of *animals* that underwent spinal deafferentation and/or bisection procedures and the number of *cycles* analyzed. Other values are expressed as target-referent mean phase ± circular SD. Small differences in mean phase were noted between some pre- and postbisection groups; *significant difference compared to prebisection, $P < 0.05$, Watson–Williams F test for circular data (Batschelet 1981; Mardia and Jupp 2000). All pre- and postbisection phase values were significantly clustered around their respective means ($P < 0.0001$, Rayleigh test; Batschelet 1981; Mardia and Jupp 2000), indicating strongly coupled interlimb coordination before and after spinal cord bisection. Abbreviations: LF, left forelimb; RF, right forelimb; LH, left hip; RH, right hip.

TABLE 2. *Limb movement amplitudes before and after cord bisections in afferented and deafferented animals*

	Animals/Cycles	Right Forelimb	Left Forelimb	Right Hip	Left Hip
			A. Afferented animals		
D8–S2 bisections					
Prebisection	1/25	100.0 ± 11.2	100.0 ± 10.0	100.0 ± 10.5	100.0 ± 15.3
Postbisection	1/25	96.5 ± 16.5	84.9 ± 12.2*	82.2 ± 14.9*	89.9 ± 15.5*
D7–S2 bisections					
Prebisection	3/75	100.0 ± 9.0	100.0 ± 8.1	100.0 ± 16.8	100.0 ± 14.5
Postbisection	3/75	100.4 ± 11.3	98.3 ± 11.6	51.5 ± 15.4*	25.1 ± 9.4*
			B. Deafferented animals		
D8–S2 bisections					
Prebisection	4/100	100.0 ± 7.7	100.0 ± 6.7	100.0 ± 30.1	100.0 ± 29.2
Postbisection	4/100	95.3 ± 10.6*	98.8 ± 9.6	40.5 ± 13.3*	61.6 ± 34.0*
D7–S2 bisections					
Prebisection	3/75	100.0 ± 8.3	100.0 ± 10.1	100.0 ± 21.3	100.0 ± 19.3
Postbisection	3/75	89.2 ± 10.3*	91.4 ± 11.2*	27.1 ± 11.7*	16.4 ± 9.2*

The mean prebisection value for each group was set at 100% and other values were expressed as percentages of their respective prebisection means. * Significant difference from prebisection, $P < 0.05$, Mann–Whitney U test. The same swim cycles were used as in Table 1.

tion between the right and left hindlimbs during swimming by splitting the cord from segments D8–S2 ($n = 5$), or D7–S2 ($n = 6$, including three turtles that previously had the D8–S2 bisection). Table 1 shows that mean interlimb phase values after D8–S2 and D7–S2 cord bisections (including afferented and deafferented turtles) changed only little compared with prebisection controls: contralateral hindlimbs (LH–RH) still displayed strong out-of-phase coordination with mean phase values close to 0.5 (range = 0.42–0.51; Table 1). Ipsilateral forelimb–hindlimb pairs (RH–RF) still exhibited mean phase values near 0.4 (range = 0.33–0.48), and diagonal limbs (LH–RF) were still nearly in phase, with mean phase values close to 1.0 (range = 0.90–0.92). Neither D8–S2 nor D7–S2 bisections weakened the out-of-phase coordination between

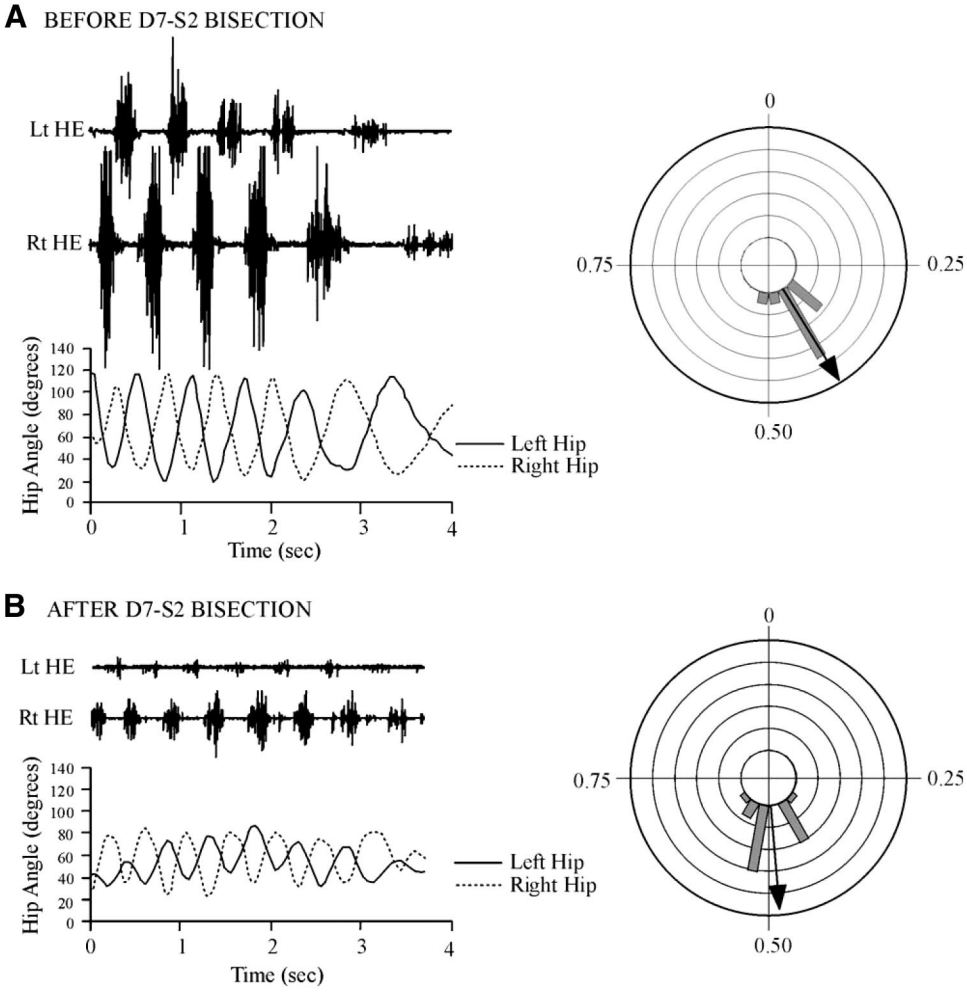

FIG. 3. D7–S2 bisections did not eliminate 1:1 hindlimb alternation, but did reduce hip movement amplitudes. Circular histograms indicate phase values for the onset of left hip extension movement within the right hip extension cycle. Gray bars extending from the innermost circle indicate the number of cycles falling within a range of phase values (bar width = 0.06). Each concentric circle represents 4 cycles for each range of phase values (from 0 to 20 cycles). Direction of vectors (arrows) indicates the mean phase, whereas vector length indicates the strength of interlimb coupling (r) on a scale of 0 (innermost circle) to 1.0 (outermost circle). *A*: kinematic and EMG data before spinal bisection show an alternation of limb movements and hip extensor (HE) EMG bursts on the right (Rt) and left (Lt) sides. Peak HE muscle activity occurred just before peak hip extension (maximum hip angle) in a given limb. First swim cycle for this episode is not shown. Mean interlimb phase = 0.41, $r = 0.97$, $P < 0.0001$ (Rayleigh test). *B*: after a D7–S2 cord bisection, 1:1 alternation of the right and left hips is maintained, but movement amplitudes are significantly reduced compared with prebisection controls. Mean phase = 0.49, $r = 0.94$, $P < 0.0001$ (Rayleigh test).

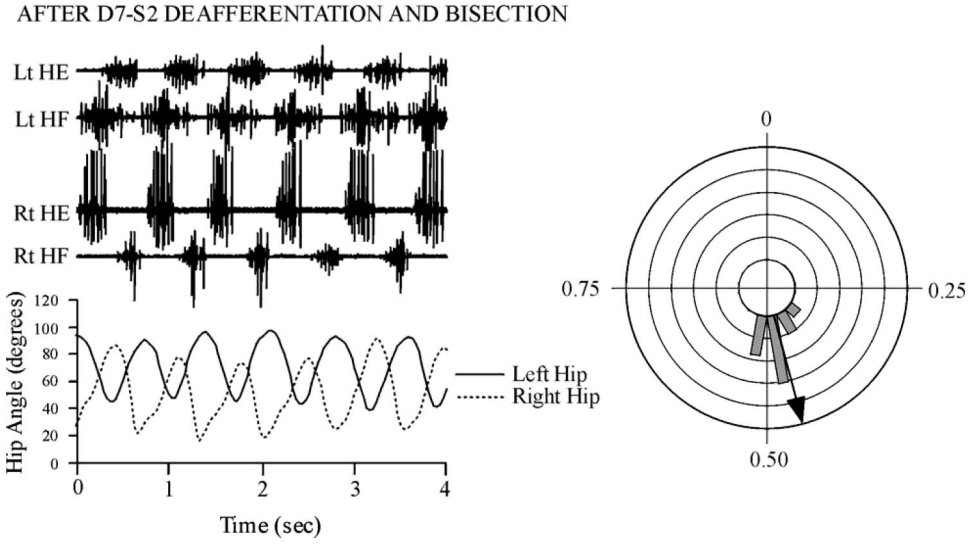

FIG. 4. Bisection and bilateral deafferentation of segments D7–S2 did not prevent 1:1 hindlimb alternation during forward swimming. Hip flexor (HF) and hip extensor (HE) EMGs are shown with kinematic data. As in Fig. 3, the circular histogram indicates phase values for the onset of left hip extension within the right hip extension cycle, using the same units. Mean interlimb phase = 0.46, $r = 0.98$, $P < 0.0001$ (Rayleigh test). Prebisection swimming is not shown.

contralateral hindlimbs (hips), nor did these lesions affect the strength of phase coupling between other limbs, including contralateral forelimbs, or forelimb–hindlimb pairs (ipsilateral and contralateral) (Table 1; Figs. 3 and 4). Although a subset of mean phase values showed small but significant differences from prebisection controls (Watson–Williams test, $P < 0.05$) (Table 1), interlimb coordination remained very strong after bisection because all four phase distributions (LH–RH, LF–RF, RH–RF, and LH–RF) were significantly clustered (nonuniform) for every turtle (Rayleigh test, $P < 0.0001$). Strong interlimb coupling after cord bisection was also indicated by vector lengths close to 1.0 (LH–RH: 0.81–0.97; RH–RF: 0.86–0.97; LH–RF: 0.69–0.95). As stated previously (see METHODS), one turtle was deafferented after D7–S2 bisection. In this case, LH–RH coordination postbisection, predeafferentation, and postdeafferentation remained out of phase (predeafferentation: 0.48 ± 0.06; postdeafferentation: 0.43 ± 0.07) and strongly coupled (Rayleigh test, $P < 0.0001$). Although we wanted to confine our studies to forward swimming, turtles commonly displayed head angles greater than 10° accompanied by turning behavior, although turning was rarely vigorous enough to observe bilateral hindlimb movements postbisection. When bilateral movements were present, even in deafferented animals, we observed 1:1, qualitatively out-of-phase right–left hindlimb coordination, similar to previous observations in intact turtles (Field and Stein 1997).

In five turtles, EMGs were recorded from selected hindlimb muscles to verify that the often small-amplitude postbisection swimming movements of the hips were attributable to active muscle contractions rather than being caused by passive mechanical coupling to other moving limbs. During pre- and postbisection swimming, EMG and motion analysis data were qualitatively correlated, with HE onsets occurring near the minimum hip angle for each cycle and HF onsets occurring near the maximum hip angle for each cycle (Fig. 4). Hip extensor EMG bursts on the right and left sides continued to exhibit strict alternation after D7–S2 cord bisection (Figs. 3 and 4).

We also tested the possibility that phasic sensory inputs, resulting from weak passive movement, were responsible for maintaining postbisection coordination of the right and left hindlimbs by triggering reflex muscle contractions within the moving limbs. Spinal segments D8–S2 ($n = 1$) or D7–S2 ($n = 5$; see METHODS) were deafferented by bilateral dorsal rhizotomy. Deafferentation did not eliminate or reduce the strongly coupled out-of-phase coordination between right and left hindlimbs (LH–RH), nor did it affect the coupling between other limb pairs (Table 1; Fig. 4). This indicated that postbisection interlimb coordination was maintained by CNS synaptic connections alone.

AMPLITUDE ANALYSIS. Although splitting the cord from D8–S2 or D7–S2 had surprisingly little effect on right–left hindlimb coordination, these lesions did significantly reduce the *amplitude* of hip movements and hip extensor EMG bursts on both sides (Mann–Whitney *U* test, $P < 0.05$) (Table 2, Fig. 3). D7–S2 bisections produced much greater deficits than D8–S2 bisections in hip movement amplitudes. Furthermore, if a turtle had previously received a D8–S2 bisection, extending the bisection anteriorly one more segment, through D7, always reduced the mean hip amplitude further ($n = 3$). These effects of cord bisection were more pronounced in deafferented turtles (D7–S2 dorsal roots cut before obtaining prebisection control data) than in afferented turtles (D7–S2 dorsal roots intact). Hindlimb movement deficits were not the result of a general postsurgical sluggishness (which should affect hindlimbs and forelimbs similarly) because hindlimb amplitudes decreased significantly more than right or left forelimb amplitudes (Mann–Whitney *U* test, $P < 0.001$) in all but one animal (afferented D8–S2 bisection, in which RF vs. LH, LF vs. RH, and LF vs. LH were all *not* significantly different; $P > 0.05$). Because we assessed only carapace-restrained animals, it is unclear whether the deficits we observed in hindlimb movement amplitude would have prevented effective swimming in freely behaving (unrestrained) turtles.

DISCUSSION

Our data show that absolute (1:1) out-of-phase coordination of the hindlimbs was maintained in voluntarily swimming turtles after midsagittal bisections of the spinal hindlimb enlargement (D8–S2) and first preenlargement segment (D7) that completely severed commissural fibers and separated the right

and left halves of the posterior spinal cord. Despite smaller-amplitude movements, strict alternation of right and left hindlimb swimming movements and hip EMG activity continued even after bisection and bilateral deafferentation of D7–S2 (Figs. 3 and 4, Table 1), indicating that the coordination was maintained by central signals originating anterior to D7 and not by commissural axons in or near the hindlimb enlargement or by movement-triggered sensory reflexes. These results show that commissural fibers in and near the hindlimb enlargement are not required for right–left hindlimb alternation during voluntary swimming and demonstrate the existence of redundant coordinating mechanisms. We suggest that descending propriospinal drive from rhythmically active locomotor circuitry in the spinal forelimb enlargement maintains the out-of-phase coordination of right and left hindlimbs in the bisected-cord preparation.

Commissural pathways in turtle hindlimb enlargement can mediate right–left coordination in some circumstances

There is ample evidence that commissural pathways in the turtle spinal cord can contribute to right–left hindlimb coordination under certain conditions. Many studies with low-spinal immobilized turtles have observed coordinated right–left alternation in hindlimb motor output during unilaterally and bilaterally evoked fictive scratching (Currie and Gonsalves 1997, 1999; Currie and Lee 1997; Currie and Stein 1989; Stein et al. 1995, 1998). Crossed inhibitory and excitatory effects were also observed in low-spinal immobilized turtles during fictive flexion reflex (Currie and Lee 1996) and during interactions between fictive flexion reflex and contralateral scratch motor patterns (Currie and Stein 1989). Because these turtles were low-spinal, with no possible contribution from the disconnected forelimb enlargement, commissural axons within the hindlimb enlargement and/or preenlargement segments must have mediated the crossed motor effects and coordination. Additional experiments showed out-of-phase coupling of right and left side rhythmic motor discharge elicited by bath-applied α-amino-3-hydroxy-5-methyl-4-isoxazolepropionic acid (AMPA) or *N*-methyl-D-aspartate (NMDA) in isolated preparations of the D7–D8 turtle spinal cord (Currie 1999) and scratchlike fictive motor patterns evoked by cutaneous nerve stimulation in isolated D8 preparations (Currie and Lee 1996), thus demonstrating functional crossed coordinating mechanisms in these segments. Intracellular recording, combined with Neurobiotin injections, has been used successfully to identify subsets of spinal interneurons in the turtle hindlimb enlargement that possess crossed axons within the enlargement and are active during one or more forms of fictive scratch and flexion reflex (Berkowitz 2005; Berkowitz et al. 2006). Such cells may contribute to right–left coupling.

Of course, extensive evidence from other vertebrate preparations shows that commissural pathways play important roles in maintaining right–left phase coupling, although the data come largely from isolated spinal cord or semiintact preparations in which locomotor activity was artificially activated. Midsagittal sectioning of isolated neonatal rat spinal cords from segments L3–L6 or Th12–L2 greatly reduced the right–left coupling of 5-HT/NMDA-induced lumbar ventral root bursts, even when these lesions were limited to the ventral commissure (Kjaerulff and Kiehn 1996). In lampreys, various lesion studies have suggested essential roles for commissural pathways in right–left alternation by using midline bisections of isolated-cord or semiintact-immobilized preparations (see Fig. 5 in Cangiano and Grillner 2003; see Fig. 6 in Jackson et al. 2005), midline bisections of moving preparations (see Fig. 4 in Jackson et al. 2005), photoablation of commissural interneurons (Buchanan and McPherson 1995), or strychnine blockade of glycinergic synapses, which converted right–left motor output from alternating to synchronized (Cohen and Harris-Warrick 1984; Hagevik and McClellan 1994).

Longitudinal propriospinal pathways mediate forelimb–hindlimb coordination

Past in vivo experiments suggested that turtle forelimb–hindlimb coordination was maintained at least in part by propriospinal pathways. The fact that high-spinal turtles produce coordinated forelimb–hindlimb motor output in response to unpatterned electrical stimulation of the cervical dorsolateral funiculus (DLF) (Stein 1978) showed that forelimb–hindlimb coordination did not depend on supraspinal input. Studies involving electrical brain stem stimulation in decerebrate-immobilized turtles (Currie 2003) indicated that sensory input was also not required for proper forelimb–hindlimb coordination during fictive swimming. Alternating activity in the forelimb enlargement may entrain alternating hindlimb activity by descending propriospinal axons. This is supported by recent mammalian studies. For example, Akay et al. (2006) showed in decerebrate cats walking on a laterally split treadmill (separate treadmills for the forelimbs and hindlimbs) that lowering forelimb treadmill speed reduced the step frequencies of both forelimbs and hindlimbs, whereas lowering hindlimb treadmill speed affected only the hindlimb step frequency. This suggested that interlimb coordination was predominantly maintained by a descending inhibitory pathway. At present, we cannot say whether the propriospinal pathways that coordinate forelimb and hindlimb movements in turtles are crossed (coupling diagonal limbs), uncrossed (coupling ipsilateral limbs), or both; however, work by Orsal et al. (1990) indicated that forelimb and hindlimb networks interact primarily by crossed coupling between diagonal limbs during treadmill stepping in thalamic cats.

Longitudinal propriospinal pathways can mediate right–left coordination

Although most studies examining the role of commissural pathways in producing rhythmic, coordinated output used pharmacological or electrical stimulation of locomotor-like activity in surgically reduced preparations, our experiments assessed the role of commissural pathways in the *voluntary* locomotion of largely intact animals. In reduced preparations, it is possible that some descending pathways, which may be sufficient to maintain right–left alternation, are eliminated. As far as we can determine, the only other in vivo study indicating that longitudinal propriospinal tracts can contribute to right–left hindlimb coordination was conducted in cats, where midsagittal bisections of the lumbar cord did not disrupt right–left hindlimb alternation during voluntary walking in otherwise intact animals (Kato 1988).

Various in vitro preparations also provide evidence that spinal commissural pathways are not necessary for right–left

alternation. The thoracolumbar cord of neonatal rat pups produced alternating bilateral ventral root output during 5-HT or 5-HT/NMDA-evoked fictive locomotion, even after midsagittal cord bisections from the thoracolumbar junction through the lumbar enlargement. This implied that descending supralumbar input was sufficient to maintain side-to-side alternation of the lumbar ventral roots (Cowley and Schmidt 1997; Kremer and Lev-Tov 1997). Similar experiments in larval lampreys, using both whole animal and in vitro brain–spinal cord preparations, showed that descending drive from brain locomotor centers and intact, rhythmically active regions of the rostral spinal cord, could drive rhythmic locomotor output from both sides of the midsagittally split caudal spinal cord (right and left caudal hemicords) (Jackson et al. 2005). In turtles, Kusuma and ten Donkelaar (1980) histologically traced the cell bodies and axon terminals of long propriospinal axons that interconnected the limb enlargements, suggesting that these fibers contributed to interlimb coordination. A subset of long descending propriospinal axons that traveled in the ventral and lateral funiculi at midbody originated from cell bodies in the ventral gray matter of the forelimb enlargement and terminated in the ventral and intermediate gray of the hindlimb enlargement. Evidence from our laboratory (Samara and Currie 2004; unpublished observations) showed that unilateral lesions of this ventrolateral white matter in the interenlargement region of the turtle spinal cord disrupted *both* ipsilateral forelimb–hindlimb coordination *and* hindlimb–hindlimb coordination during voluntary swim behavior. The effect on hindlimb–hindlimb coordination may have been due to the disrupted balance of descending propriospinal drive to the right and left hindlimb circuitry.

Significance of reduced hindlimb (hip) swim amplitudes after bisection of the D7 segment

In addition to indicating that descending propriospinal drive alone can maintain right–left hindlimb coordination, our results may provide insight into how descending pathways that excite spinal locomotor CPGs ("locomotor command pathways") are organized in turtles to activate contralateral hindlimb movements. As shown in Table 2, D7–S2 bisections decreased hindlimb swim amplitudes much more than D8–S2 bisections. One possible explanation is that bisection of the D7 segment cuts a major fraction of the descending locomotor command where it crosses the midline anterior to the D8–S2 hindlimb enlargement. This is consistent with previous evidence showing that electrical stimulation of the right D3 DLF in low-spinal turtles with movement continued to evoke swimlike movements in the *left* hindlimb after surgical removal of the right side of the segments D8–S2 (Samara and Currie 2006). Another spinal lesion study in low-spinal immobilized turtles suggested that these command pathways cross the midline posterior to the D5 spinal segment (Currie 2000). Thus it is likely that the crossed locomotor command tracts that have been demonstrated in several turtle preparations (decerebrate with movement: Kazzenikov et al. 1980; decerebrate immobilized: Currie 2003; high-spinal with movement: Stein 1978; low-spinal with movement: Lennard and Stein 1977; low-spinal immobilized: Juranek and Currie 2000; voluntarily swimming intact: Samara and Currie 2004) activate contralateral hindlimb locomotion by a pathway that crosses the midline largely within segments D7 and/or D6, just anterior to the hindlimb enlargement. Further experiments are required to identify the cells of origin and characterize the timing and spatial distribution of descending axonal signals that turn on and modulate turtle locomotion.

Can descending propriospinal drive originating in the forelimb enlargement directly activate hindlimb motor output?

The low-amplitude hindlimb movements and hip EMG bursts that continued after we split the lumbosacral cord from D7–S2 may have been activated *1*) by surviving command fibers (uncrossed or crossing anterior to D7) that were left intact by the spinal bisection, *2*) by the same descending propriospinal signals from the forelimb enlargement that also coordinated forelimb and hindlimb movements, or *3*) a combination of both. What is the evidence that interenlargement propriospinal activity by itself can directly drive motor output? In isolated and partitioned neonatal rat spinal cords, descending 5-HT or 5-HT/NMDA-induced drive originating in the cervical enlargement was demonstrated to be sufficient to induce fictive locomotor output from the hindlimb enlargement (Ballion et al. 2001). In our future experiments, similar studies with in vitro turtle spinal cords that include both limb enlargements could determine the extent to which localized, chemically activated locomotor activity in the forelimb enlargement can directly drive hindlimb motor discharge.

GRANTS

This research was supported by National Science Foundation Grant IBN-0316240 to S. N. Currie.

REFERENCES

Akay T, McVea DA, Tachibana A, Pearson KG. Coordination of fore and hind leg stepping in cats on a transversely-split treadmill. *Exp Brain Res* 175: 211–222, 2006.

Ballion B, Morin D, Viala D. Forelimb locomotor generators and quadrupedal locomotion in the neonatal rat. *Eur J Neurosci* 14: 1727–1738, 2001.

Batschelet E. *Circular Statistics in Biology*. London: Academic Press, 1981.

Berkowitz A. Physiology and morphology indicate that individual spinal interneurons contribute to diverse limb movements. *J Neurophysiol* 94: 4455–4470, 2005.

Berkowitz A, Stein PSG. Activity of descending propriospinal axons in the turtle hindlimb enlargement during two forms of fictive scratching: phase analyses. *J Neurosci* 14: 5105–5119, 1994.

Berkowitz A, Yosten GLC, Ballard MR. Somato-dendritic morphology predicts physiology for neurons that contribute to several kinds of limb movements. *J Neurophysiol* 95: 2821–2831, 2006.

Buchanan JT, McPherson DR. The neuronal network for locomotion in the lamprey spinal cord: evidence for the involvement of commissural interneurons. *J Physiol* (*Paris*) 89: 221–233, 1995.

Butt SJ, Lebret JM, Kiehn O. Organization of left–right coordination in the mammalian locomotor network. *Brain Res Rev* 40: 107–117, 2002.

Cangiano L, Grillner S. Fast and slow locomotor burst generation in the hemispinal cord of the lamprey. *J Neurophysiol* 89: 2931–2942, 2003.

Cohen AH, Harris-Warrick RM. Strychnine eliminates alternating motor output during fictive locomotion in the lamprey. *Brain Res* 293: 164–167, 1984.

Cowley KC, Schmidt BJ. Regional distribution of the locomotor pattern-generating network in the neonatal rat spinal cord. *J Neurophysiol* 77: 247–259, 1997.

Currie SN. Fictive hindlimb motor patterns evoked by AMPA and NMDA in turtle spinal cord-hindlimb nerve preparations. *J Physiol* (*Paris*) 93: 199–211, 1999.

Currie SN. Descending pathways that activate fictive swim motor patterns in the turtle spinal cord. *Soc Neurosci Abstr* 26: 746.1, 2000.

Currie SN. Fictive locomotion evoked by electrical stimulation of the brainstem in decerebrate immobilized turtles. *Soc Neurosci Abstr* 29: 276.9, 2003.

Currie SN, Gonsalves GG. Right–left interactions between rostral scratch networks generate rhythmicity in the preenlargement spinal cord of the turtle. *J Neurophysiol* 78: 3479–3483, 1997.

Currie SN, Gonsalves GG. Reciprocal interactions in the turtle hindlimb enlargement contribute to scratch rhythmogenesis. *J Neurophysiol* 81: 2977–2987, 1999.

Currie SN, Lee S. Glycinergic inhibition in the turtle spinal cord regulates the intensity and pattern of fictive flexion reflex motor output. *Neurosci Lett* 205: 75–78, 1996.

Currie SN, Lee S. Glycinergic inhibition contributes to the generation of rostral scratch motor patterns in the turtle spinal cord. *J Neurosci* 17: 3322–3333, 1997.

Currie SN, Stein PSG. Interruptions of fictive scratch motor rhythms by activation of cutaneous flexion reflex afferents in the turtle. *J Neurosci* 9: 488–496, 1989.

Davenport J, Munks SA, Oxford PJ. A comparison of swimming in marine and freshwater turtles. *Proc R Soc Lond B Biol Sci* 220: 447–475, 1984.

Delvolve I, Bem T, Cabelguen JM. Epaxial and limb muscle activity during swimming and terrestrial stepping in the adult newt *Pleurodeles waltl*. *J Neurophysiol* 78: 638–650, 1997.

Earhart GM, Stein PSG. Step, swim, and scratch motor patterns in the turtle. *J Neurophysiol* 84: 2181–2190, 2000.

English AW. Interlimb coordination during stepping in the cat: an electromyographic analysis. *J Neurophysiol* 42: 229–243, 1979.

Field EC, Stein PSG. Spinal cord coordination of hindlimb movements in the turtle: interlimb temporal relationships during bilateral scratching and swimming. *J Neurophysiol* 78: 1404–1413, 1997.

Gillis GB, Blob RW. How muscles accommodate movement in different physical environments: aquatic vs. terrestrial locomotion in vertebrates. *Comp Biochem Physiol A Physiol* 131: 61–75, 2001.

Grillner S. Control of locomotion in bipeds, tetrapods, and fish. In: *Handbook of Physiology. The Nervous System. Motor Control*. Bethesda, MD: Am. Physiol. Soc., 1981, sect. 1, vol. II, pt. 2, p. 1179–1236.

Hagevik A, McClellan AD. Coupling of spinal locomotor networks in larval lamprey revealed by receptor blockers for inhibitory amino acids: neurophysiology and computer modeling. *J Neurophysiol* 72: 1810–1829, 1994.

Hildebrand M. The quadrupedal gaits of vertebrates. *Bioscience* 39: 766–775, 1989.

Jackson AW, Horinek DF, Boyd MR, McClellan AD. Disruption of left–right reciprocal coupling in the spinal cord of larval lamprey abolishes brain-initiated locomotor activity. *J Neurophysiol* 94: 2031–2044, 2005.

Jacobson RD, Hollyday M. Electrically evoked walking and fictive locomotion in the chick. *J Neurophysiol* 48: 257–270, 1982.

Jovanovic K, Petrov T, Stein RB. Effects of inhibitory neurotransmitters on the mudpuppy (*Necturus maculatus*) locomotor pattern in vitro. *Exp Brain Res* 129: 172–184, 1999.

Juranek J, Currie SN. Electrically evoked fictive swimming in the low-spinal immobilized turtle. *J Neurophysiol* 83: 146–155, 2000.

Juvin L, Simmers J, Morin D. Propriospinal circuitry underlying interlimb coordination in mammalian quadrupedal locomotion. *J Neurosci* 25: 6025–6035, 2005.

Kahn JA, Roberts A. Experiments on the central pattern generator for swimming in amphibian embryos. *Philos Trans R Soc Lond B Biol Sci* 296: 229–243, 1982.

Kahn JA, Roberts A, Kashin SM. The neuromuscular basis of swimming movements in embryos of the amphibian *Xenopus laevis*. *J Exp Biol* 99: 175–184, 1982.

Kato M. Longitudinal myelotomy of lumbar spinal cord has little effect on coordinated locomotor activities of bilateral hindlimbs of the chronic cats. *Neurosci Lett* 93: 259–263, 1988.

Kazzenikov OV, Selionov VA, Shik ML, Iakovleva GV. Rhombencephalic "locomotor area" of turtles (in Russian). *Neirofiziologiia* 12: 382–390, 1980.

Kiehn O. Locomotor circuits in the mammalian spinal cord. *Annu Rev Neurosci* 29: 279–306, 2006.

Kjaerulff O, Kiehn O. Distribution of networks generating and coordinating locomotor activity in the neonatal rat spinal cord *in vitro*: a lesion study. *J Neurosci* 16: 5777–5794, 1996.

Kremer E, Lev-Tov A. Localization of the spinal network associated with generation of hindlimb locomotion in the neonatal rat and organization of its transverse coupling system. *J Neurophysiol* 77: 1155–1170, 1997.

Kusuma A, ten Donkelaar HJ. Propriospinal fibers interconnecting the spinal enlargements in some quadrupedal reptiles. *J Comp Neurol* 193: 871–891, 1980.

Lennard PR, Stein PS. Swimming movements elicited by electrical stimulation of turtle spinal cord. I. Low-spinal and intact preparations. *J Neurophysiol* 40: 768–778, 1977.

Mardia KV, Jupp PE. *Directional Statistics* (2nd ed.). New York: Wiley, 2000.

Masino MA, Fetcho JR. Fictive swimming motor patterns in wild type and mutant larval zebrafish. *J Neurophysiol* 93: 3177–3188, 2005.

McPherson DR, Buchanan JT, Kasicki S. Effects of strychnine of fictive swimming in the lamprey: evidence for glycinergic inhibition, discrepancies with model predictions, and novel modulatory rhythms. *J Comp Physiol A Sens Neural Behav Physiol* 175: 311–321, 1994.

Miller S, Vanderburg J, van der Meche FGA. Locomotion in cat: basic programs of movement. *Brain Res* 91: 239–253, 1975.

Mortin LI, Stein PSG. Spinal cord segments containing key elements of the central pattern generators for three forms of scratch reflex in the turtle. *J Neurosci* 9: 2285–2296, 1989.

Orsal D, Cabelguen JM, Perret C. Interlimb coordination during fictive locomotion in the thalamic cat. *Exp Brain Res* 82: 536–546, 1990.

Ostry DJ, Feldman AG, Flanagan JR. Kinematics and control of frog hindlimb movements. *J Neurophysiol* 65: 547–562, 1991.

Peters SE, Kamel LT, Bashor DP. Hopping and swimming in the leopard frog, *Rana pipiens*: I. Step cycles and kinematics. *J Morphol* 230: 1–16, 1996.

Roberts A, Soffe SR, Wolf ES, Yoshida M, Zhao FY. Central circuits controlling locomotion in young frog tadpoles. *Ann NY Acad Sci* 860: 19–34, 1998.

Robertson GA, Mortin LI, Keifer J, Stein PSG. Three forms of the scratch reflex in the spinal turtle: central generation and motor patterns. *J Neurophysiol* 53: 1517–1534, 1985.

Samara RF, Currie SN. Impairment of voluntary locomotion in turtles following partial lesions of the mid-body spinal cord. *Soc Neurosci Abstr* 882.12, 2004.

Samara RF, Currie SN. Crossed commissural pathways in the spinal hindlimb enlargement are not necessary for right–left hindlimb alternation during turtle swimming. *Soc Neurosci Abstr* 630.18, 2005.

Samara RF, Currie SN. Electrical activation of hindlimb locomotor activity in the turtle spinal cord hemi-enlargement preparation. *Soc Neurosci Abstr* 32: 448.27, 2006.

Sholomenko GN, Funk GD, Steeves JD. Locomotor activities in the decerebrate bird without phasic afferent input. *Neuroscience* 40: 257–266, 1991.

Soffe SR, Roberts A. Tonic and phasic synaptic input to spinal cord motoneurons during fictive locomotion if frog embryos. *J Neurophysiol* 48: 1279–1288, 1982.

Stein PSG. Swimming movements elicited by electrical stimulation of the turtle spinal cord: the high spinal preparation. *J Comp Physiol A Sens Neural Behav Physiol* 124: 203–210, 1978.

Stein PSG. Neuronal control of turtle hindlimb motor rhythms. *J Comp Physiol A Sens Neural Behav Physiol* 191: 213–229, 2005.

Stein PSG, Grillner S, Selverston AI, Stuart DG. *Neurons, Networks, and Motor Behavior*. Cambridge, MA: MIT Press, 1997.

Stein PSG, McCullough ML. Example of 2:1 interlimb coordination during fictive rostral scratching in a spinal turtle. *J Neurophysiol* 79: 1132–1134, 1998.

Stein PSG, McCullough ML, Currie SN. Spinal motor patterns in the turtle. *Ann NY Acad Sci* 860: 142–154, 1998a.

Stein PSG, McCullough ML, Currie SN. Reconstruction of flexor/extensor alternation during fictive rostral scratching by two-site stimulation in the spinal turtle with a transverse spinal hemisection. *J Neurosci* 18: 467–479, 1998b.

Stein PSG, Victor JC, Field EC, Currie SN. Bilateral control of hindlimb scratching in the spinal turtle: contralateral spinal circuitry contributes to the normal ipsilateral motor pattern of fictive rostral scratching. *J Neurosci* 15: 4343–4355, 1995.

Walker WF. A structural and functional analysis of walking in the turtle, *Chrysemys picta marginata*. *J Morphol* 134: 195–214, 1971.

Walker WF Jr. The locomotor apparatus of Testudines. In: *Biology of the Reptilia*, edited by Gans C. New York: Academic Press, 1973, vol. 4, p. 1–100.

Webster KN, Dawson TJ. Locomotion energetics and gait characteristics of a rat-kangaroo, *Bettongia penicillata*, have some kangaroo-like features. *J Comp Physiol B Biochem Syst Environ Physiol* 173: 549–557, 2003.

Zar JH. *Biostatistical Analysis* (4th ed.). Upper Saddle River, NJ: Prentice Hall, 1999.

Zug GR. Buoyancy, locomotion, morphology of the pelvic girdle and hindlimbs, and systematics of cryptodiran turtles. *Misc Publ Mus Zool Univ Mich* 142: 1–98, 1971.